Application of simple all-sky imagers for the estimation of aerosol optical depth

Andreas Kazantzidis, Panagiotis Tzoumanikas, Efterpi Nikitidou, Vasileios Salamalikis, Stefan Wilbert, and Christoph Prahl

Citation: AIP Conference Proceedings **1850**, 140012 (2017);

View online: https://doi.org/10.1063/1.4984520

View Table of Contents: http://aip.scitation.org/toc/apc/1850/1

Published by the American Institute of Physics

Articles you may be interested in

Solar energy incident at the receiver of a solar tower plant, derived from remote sensing: Computation of both DNI and slant path transmittance
AIP Conference Proceedings **1850**, 140005 (2017); 10.1063/1.4984513

Atmospheric extinction in simulation tools for solar tower plants
AIP Conference Proceedings **1850**, 140011 (2017); 10.1063/1.4984519

Short-term forecasting of high resolution local DNI maps with multiple fish-eye cameras in stereoscopic mode
AIP Conference Proceedings **1850**, 140004 (2017); 10.1063/1.4984512

Atmospheric transmission loss in mirror-to-tower slant ranges due to water vapor
AIP Conference Proceedings **1850**, 140010 (2017); 10.1063/1.4984518

A methodology for probabilistic assessment of solar thermal power plants yield
AIP Conference Proceedings **1850**, 140006 (2017); 10.1063/1.4984514

Applicability of ASHRAE clear-sky model based on solar-radiation measurements in Saudi Arabia
AIP Conference Proceedings **1850**, 140001 (2017); 10.1063/1.4984509

Application of Simple All-sky Imagers for the Estimation of Aerosol Optical Depth

Andreas Kazantzidis[1,a)], Panagiotis Tzoumanikas[1], Efterpi Nikitidou[1], Vasileios Salamalikis[1], Stefan Wilbert[2], Christoph Prahl[2]

[1]*Laboratory of Atmospheric Physics, Physics Department, University of Patras, 26500, Patras, Greece*
[2]*German Aerospace Center (DLR), Institute of Solar Research, Plataforma de Almería, Ctra. de Senés s/n km 4, 04200 Tabernas, Spain*

[a)] Corresponding author: akaza@upatras.gr

Abstract. Aerosol optical depth is a key atmospheric constituent for direct normal irradiance calculations at concentrating solar power plants. However, aerosol optical depth is typically not measured at the solar plants for financial reasons. With the recent introduction of all-sky imagers for the nowcasting of direct normal irradiance at the plants a new instrument is available which can be used for the determination of aerosol optical depth at different wavelengths. In this study, we are based on Red, Green and Blue intensities/radiances and calculations of the saturated area around the Sun, both derived from all-sky images taken with a low-cost surveillance camera at the Plataforma Solar de Almeria, Spain. The aerosol optical depth at 440, 500 and 675nm is calculated. The results are compared with collocated aerosol optical measurements and the mean/median difference and standard deviation are less than 0.01 and 0.03 respectively at all wavelengths.

INTRODUCTION

Aerosols are an important atmospheric constituent, affecting the incoming solar radiation, by absorbing and scattering processes and altering the lifetime and optical properties of clouds. They particularly reduce the incident direct normal irradiance (DNI) [1] and increase the circumsolar radiation [2] which further reduces the plant yield [3]. Thus, the accurate knowledge of aerosol optical depth (AOD) is of vital interest for concentrating solar power (CSP) plants. For financial reasons, AOD is typically not measured at the solar plants. AOD is therefore only estimated from DNI measurements which are performed at the plants. In recent years, all-sky imaging systems that take hemispherical images of the sky have been used in CSP plants to nowcast DNI. Furthermore, atmospheric scientists have used all-sky cameras to determine the AOD and these methods could be directly applicable at CSP plants. Hence, it is of interest to test the quality of AOD data derived from all-sky imagers which are used in the nowcasting systems to obtain this additional parameter without further instrumentation. For example such AOD data from all sky imaging systems can be used to determine the circumsolar radiation [4].

Olmo et al. [5], calculated the AOD at 500 nm, using the all-sky images' radiances and model estimations. The spectral radiance was retrieved from sky images using a linear pseudoinverse algorithm. Then, the aerosol or cloud optical depth at 550 nm was obtained as that which minimizes the residuals between the zenith spectral radiance retrieved from the sky images and that estimated by the radiative transfer code. The method was tested under extreme situations including the presence of nonspherical aerosol particles. The comparison of optical depths derived from the all-sky imager with those retrieved with a sun photometer operated side by side shows differences similar to the nominal error claimed in the aerosol optical depth retrievals from sun photometer networks. Cazorla et al. [6] calculated the AOD at three different wavelengths, using neural network-based models, with the radiance extracted from all-sky images, as input. It was revealed that almost 80% of the estimated AOD values at 440 nm and 675nm had a deviation less than 0.01 with respect to the CIMEL result which is the AERONET AOD's estimated

SolarPACES 2016
AIP Conf. Proc. 1850, 140012-1–140012-7; doi: 10.1063/1.4984520
Published by AIP Publishing. 978-0-7354-1522-5/$30.00

uncertainty. Another study focused on the retrieval of AOD from all-sky images is that of Huo and Lü [7]. The relationship between the radiance ratio (at 450 to 650 nm) and AOD was analyzed by numerical simulation and a look-up table approach was presented for the retrieval of AOD from the radiance ratio. When compared with AOD measurements from a collocated CIMEL radiometer, the correlation coefficient was estimated to be approximately 0.95, and the average retrieval error around 7%.

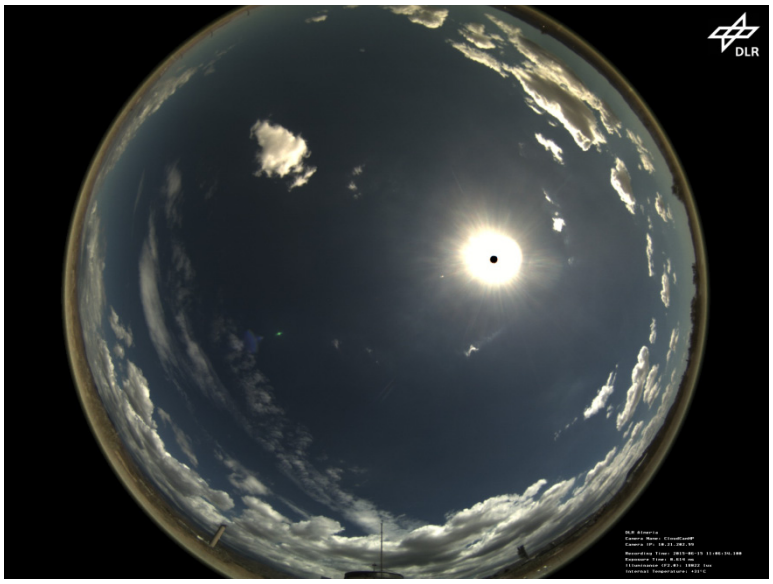

FIGURE 1. All sky image of the Q24 camera from PSA, which is used in this work.

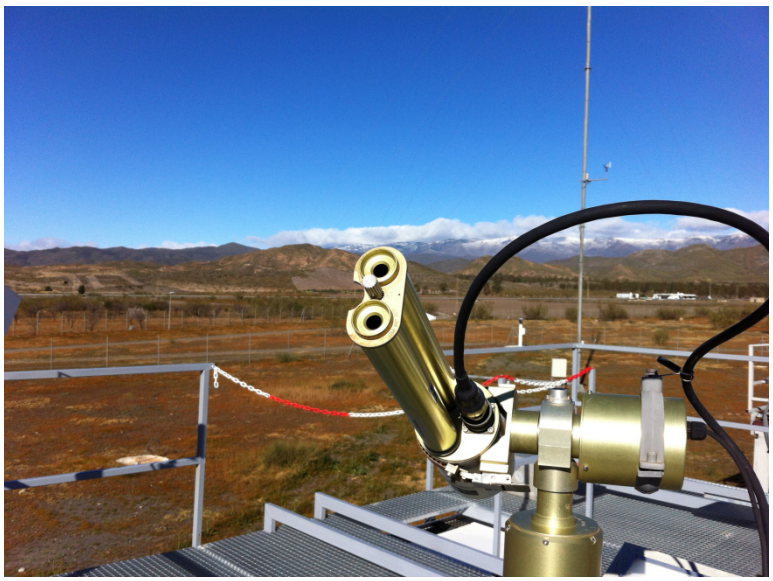

FIGURE 2. Cimel sun photometer at DLR's AERONET station "Tabernas_PSA-DLR".

In this study, AOD is calculated using a cost-efficient all-sky camera. An example image of the camera is shown in Fig. 1. In the next paragraphs, the proposed methodology is illustrated and the results are compared to the AOD from the collocated AERONET sun photometer at the Plataforma Solar de Almeria (PSA), Spain (Latitude: 37.09076° North, Longitude: 2.35818° West, Elevation: 500 m.a.m.s.l.; Fig. 2). The study was carried out in the frame of project "Direct Normal Irradiance Nowcasting methods for optimized operation of concentrating solar technologies" (DNICast, http://www.dnicast-project.net/).

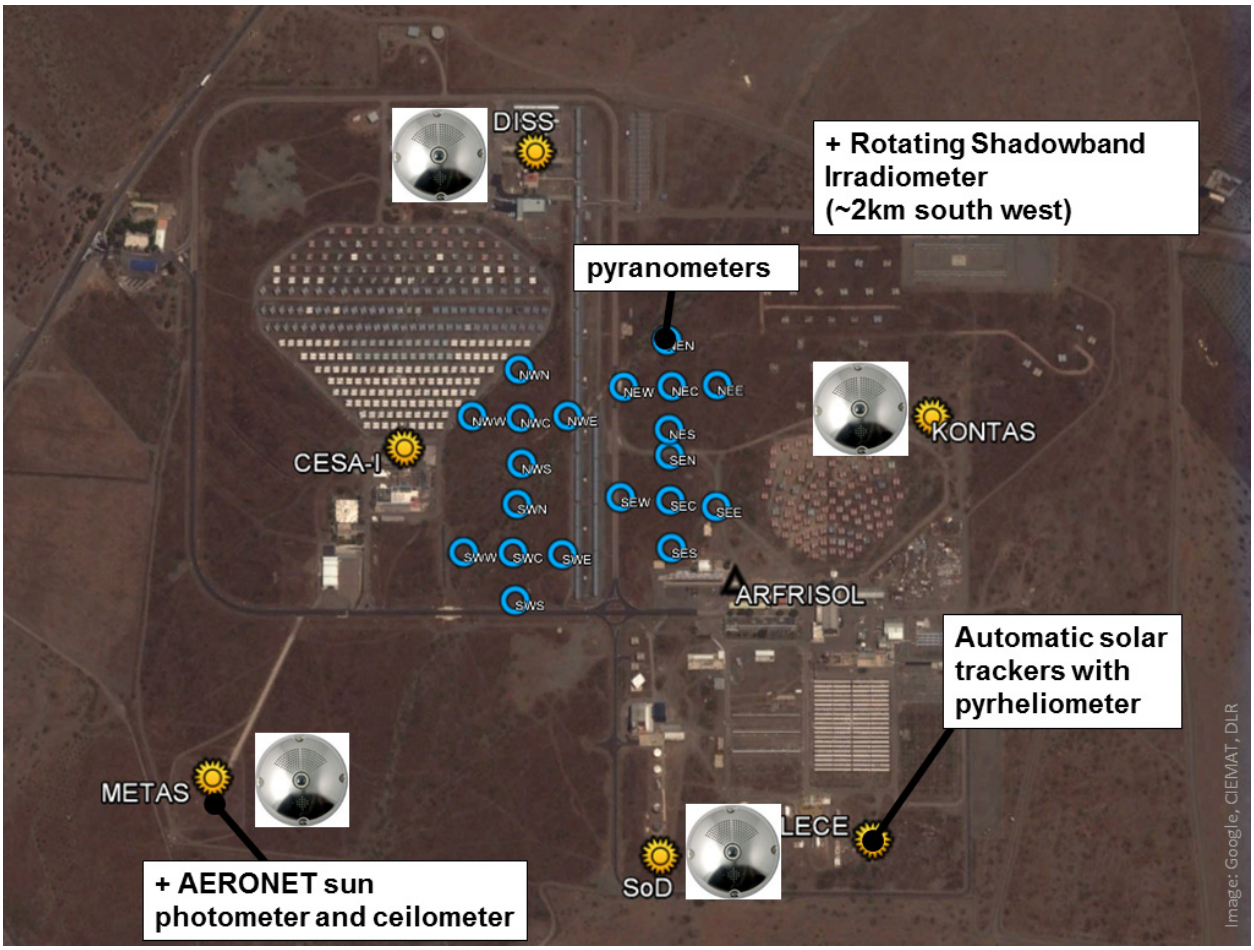

FIGURE 3. Overview of PSA sites equipped with al-sky imagers and irradiance/atmospheric measurements.

DATA AND METHODOLOGY

In the frame of DNICast, we develop and provide AOD as intermediate product of cloud camera images as a basis for an AOD nowcasting scheme. For the AOD estimations from the all sky cameras, training algorithms are developed, based on aerosol measurements from a CIMEL sun photometer (part of the AERONET network) which is available at the PSA site. An overview of the PSA site measurements is presented in Fig. 3. A bouquet of irradiance and atmospheric measurements is offered accompanied with all-sky images at four sites: DISS, METAS, SoD and KONTAS. The all sky cameras are set up next to automatic two axes trackers with ISO 9060 first class pyrheliometers and two ventilated secondary standard pyranometers (shaded and unshaded). A network of 20 Si-pyranometers with 50 m distance between the sensors collects 1 second GHI data. Next to the sun photometer also a CHM 15k ceilometer is operated. Further instrumentation such as a sunshape measurement system, a Raymetrics aerosol LIDAR, particle counters, meteorological optical range sensors and pyrheliometers with semiautomatic trackers are not shown.

Our main purpose is to analyze sky images being created and produced by Mobotix Q24M public surveillance camera in order to estimate the AOD at different wavelengths from RGB intensities (Red, Green, Blue channels) at the zenith point. Our training and test sets were taken at KONTAS site. Images of a standard exposure time (640μs) are used in order to achieve a good correlation between the change in brightness and the change in radiance for different solar zenith angles. For the training and testing of the algorithm, we use ~3500 CIMEL AOD values in synergy with the closest in time images for the period 1/6 – 21/10/2014. The measured AOD values from the AERONET level 2 dataset at 3 wavelengths (440, 500 and 675 nm) are presented in Fig. 4.

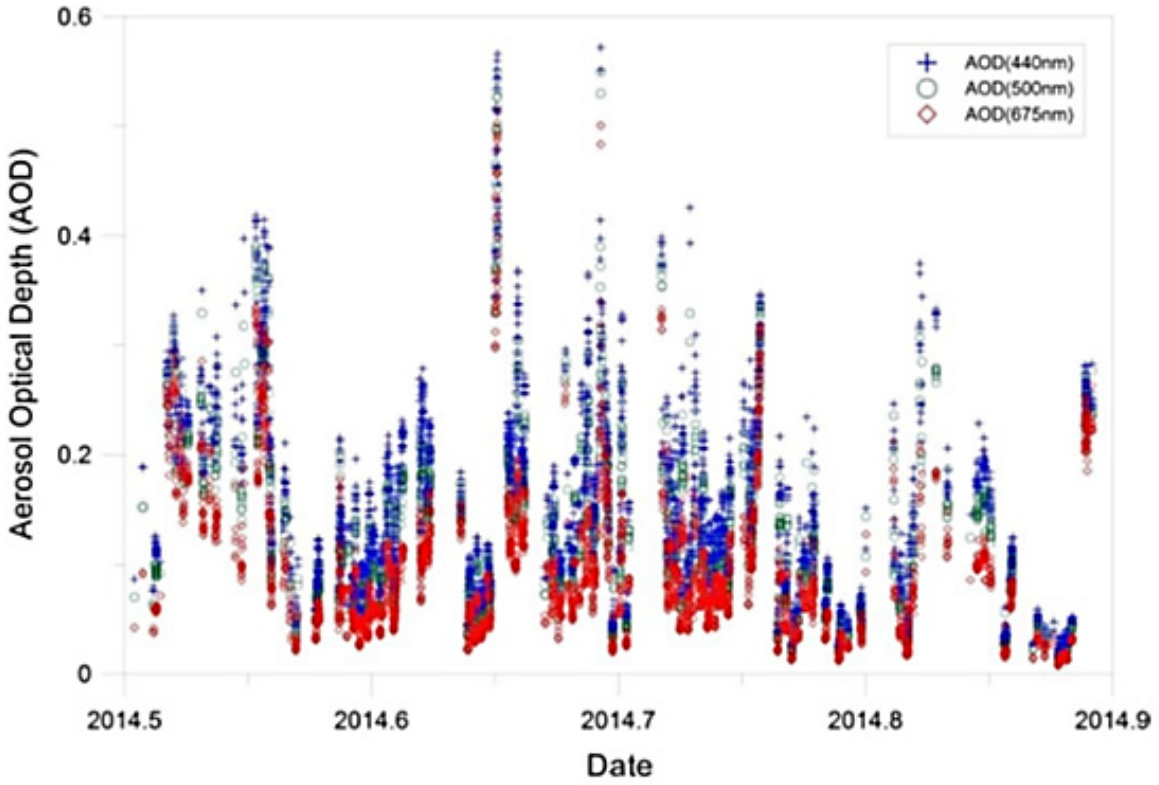

FIGURE 4. The aerosol optical depth (AOD) measurements from the AERONET level 2 dataset at 3 wavelengths (440, 500 and 675nm) at PSA for the period 1/6 – 21/10/2014.

The modeled radiances are estimated using the libRadtran software package and the UVSPEC radiative transfer model [8]. The AOD is described by the Ångström exponent α and coefficient β. The solver of the radiative transfer equation is the discrete ordinate algorithm with 64 streams considered and the sphericity of the Earth is taken into account. The RGB radiances have been calculated according to the official RGB definition. The RGB radiances were calculated for a variety of zenith (0-88^o step 2^o) and azimuth (0-180^o step 2^o) angles. In Fig. 5, the radiance values in Blue and Red are presented as a function of the Ångström coefficient β for different solar zenith angles (20, 50, 60 and 70^o). The beta values that are usually measured at the PSA site are lower than 0.4. As a result, the variability of the zenith point radiances with solar zenith angle and Ångström beta can provide adequate information in order to use this point for the estimation of the AOD.

The RGB radiance values at the zenith point depend not only from the AOD but also on other atmospheric variables, especially the precipitable water (PW) and the aerosol single scattering albedo (SSA). Based on AERONET measurements, the PW and SSA values at PSA lie between 0-30mm and 0.9-0.99 respectively. The percentage (%) changes in Red and Blue radiances (where PW and SSA are respectively expected to cause the greatest effect) are calculated for a low (20^o) and a high (70^o) solar zenith angle. According to the results, the effect of changing PW affects negligibly the zenith point Red radiance (less than 0.1%) at both solar zenith angles. The effect of changing SSA on zenith Blue radiance is expected to be less than 5%.

In order to avoid errors due to the comparably low quality of the entrance optics of the low priced camera, RGB intensities from the zenith point and one additional image parameter are used. To further reduce the discrepancies that still arise and therefore improve the quality of the AOD results, a new approach is proposed, that takes into account the saturated area around the Sun (SAT). The size of this area is dependent on the circumsolar radiation and therefore on cloudless conditions on the AOD. SAT is calculated as a percentage (%) of a greater area around the Sun, where the pixels are saturated. This multi-linear approach combines the RGB intensities at the zenith point and the SAT expressed as percentage (%) area of saturation around the Sun. The AOD is estimated at three different wavelengths, 440, 500 and 675 nm and is subsequently compared to the corresponding CIMEL measurements.

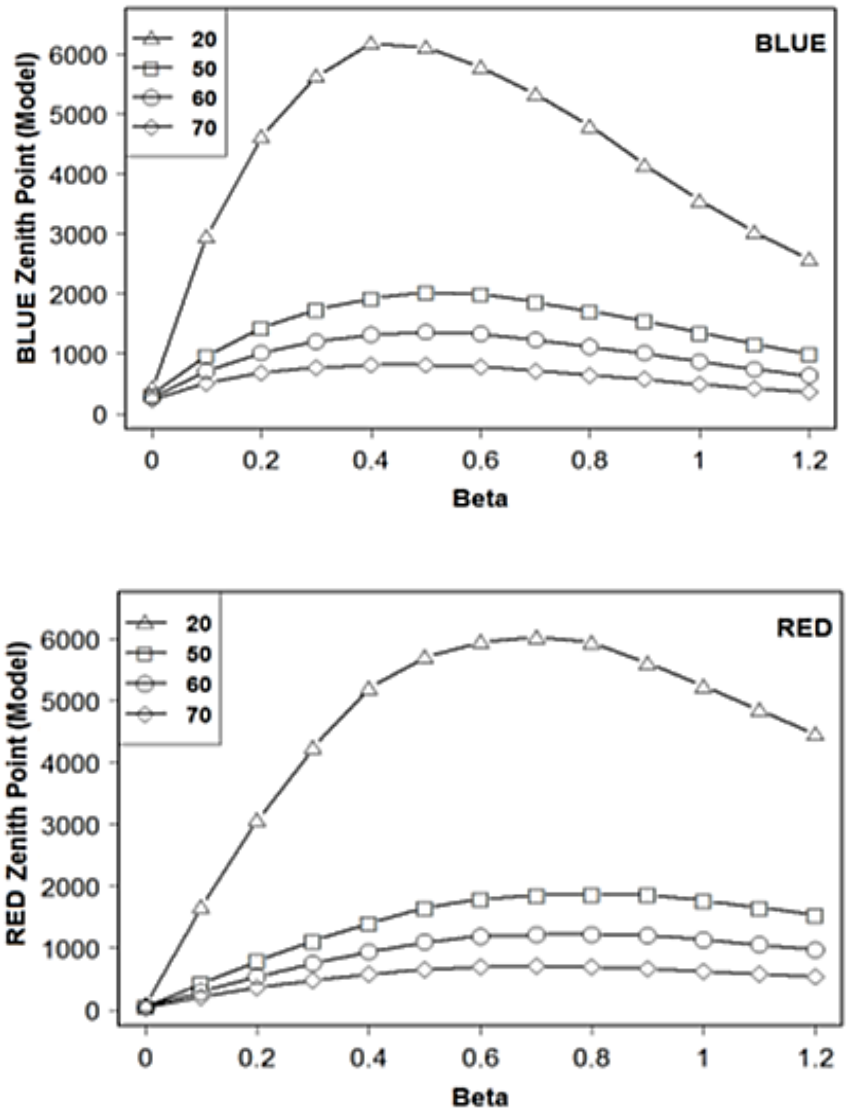

FIGURE 5. The radiance values at Blue (upper panel) and Red (lower panel) as a function of the Ångström coefficient β for different solar zenith angles (20-70^{o}).

DATA AND METHODOLOGY

Fig. 6 presents typical results from the AOD values (at 500 nm) derived from the all-sky camera and those from the sun photometer for a three months period (June-August 2014) and three solar zenith angles intervals. In addition, Table 1 shows the statistical results of these comparisons and all three wavelengths. The mean/median difference and the standard deviation are lower than 0.01 and 0.03, respectively, for all three wavelengths. The deviations are within ±0.01, in 80% of the cases. The results are comparable with those from other camera based methods and satellite-derived methodologies and provide substantial evidence that the use of simple all-sky cameras can be extended to include the efficient estimation of AOD.

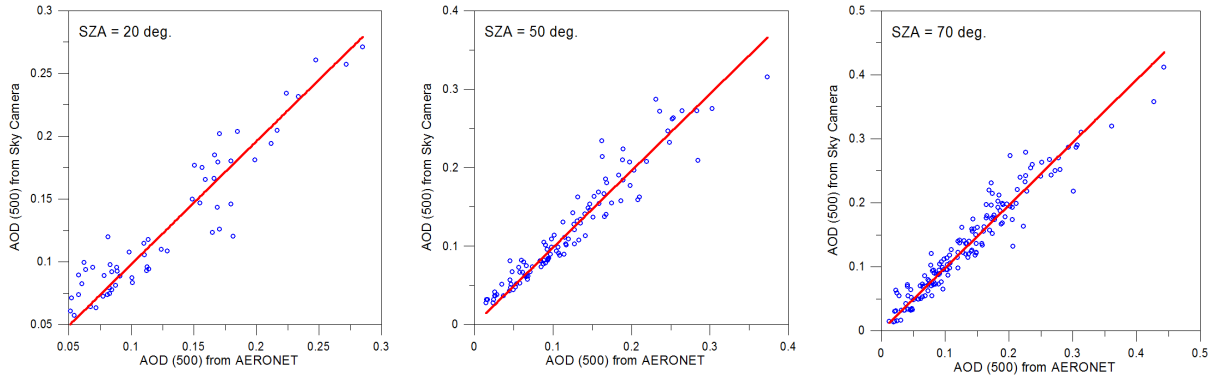

FIGURE 6. Comparison of the AOD values at 500 nm from the all-sky camera with those from the AERONET measurements for small solar zenith angles intervals centered at 20° (left panel), 50° (middle panel) and 70° (right panel).

TABLE 1. The statistical results of the differences between the estimated AOD values from the all-sky camera and the corresponding measurements from AERONET. The results are presented for 440, 500 and 675 nm.

	AOD(440 nm)	**AOD(500 nm)**	**AOD(675 nm)**
Mean differences	-0.009	0	-0.01
Median differences	-0.004	0	-0.01
Standard deviation	0.03	0.02	0.02

CONCLUSION AND PERSPECTIVES

Aerosols are considered as key atmospheric constituent for the direct normal irradiance. In recent years, efforts have been made to derive the aerosol optical properties from the analysis of the spectral characteristics of all-sky images. According to the relevant literature, the synergetic use of Red, Green, Blue intensities from the sky images, calculations from radiative transfer models and training methods are able to provide quite accurate results (error ~15-20%). The uncertainties in the retrieval of AOD are site specific and related to the sky camera type not only because of different CCD sensors but also because of using entrance optics of different quality.

The basic steps and results are listed below:

- We are based only on the RGB intensities/radiances from the zenith point and the saturated area around the sun. We prove that the variability of the zenith point radiances with solar zenith angle and Ångström coefficient β is adequate in order to use this point for the estimation of the AOD and we checked the effect of changing precipitable water and single scattering albedo. According to results, the expected changes of precipitable water and single scattering albedo at the PSA site affect RGB radiances from the zenith point by ~0.1 and 5% respectively.
- A novelty of the proposed method is the use of the saturated area around the Sun for the calculation of AOD since the size of this area is related to the circumsolar radiations and, so, with the AOD.
- Finally, both the RGB intensities at the zenith point and the percentage (%) area of saturation are taken into account in a multi-linear approach to estimate the AOD values at 440, 500 and 675nm and compared with the measurements of the CIMEL radiometer at the same wavelengths. According to results, the mean/median difference and the standard deviation are less than 0.01 and 0.03 for all wavelengths. The results are comparable with those from similar methods and satellite-derived methodologies and show that a low cost sky camera can be efficiently used for the estimation of AOD.

ACKNOWLEDGMENT

The research leading to these results has received funding from the European Union's FP7 Programme under Grant Agreement no. 608623 (DNICast project). We thank ACTRIS/AERONET for the support with the calibration and data processing of the sun photometer data.

REFERENCES

1. E. Nikitidou, A. Kazantzidis, V. Salamalikis, "The aerosol effect on direct normal irradiance under clear skies", *Renewable Energy*, **68**, 475-484 (2014).
2. Reinhardt, B., R. Buras, L. Bugliaro, S. Wilbert, and B. Mayer. 2013. "Determination of circumsolar radiation from Meteosat Second Generation." Atmos. Meas. Tech. Discuss. no. 6 (3):5835-5879. doi: 10.5194/amtd-6-5835-2013.
3. Wilbert, S., B. Reinhardt, J. DeVore, M. Röger, R. Pitz-Paal, C. Gueymard, and R. Buras. 2013. "Measurement of Solar Radiance Profiles With the Sun and Aureole Measurement System." Journal of Solar Energy Engineering no. 135 (4):041002-041002. doi: 10.1115/1.4024244.
4. Bugliaro, Luca, Stefan Wilbert, and Andreas Kazantzidis. 2016. Derivation and forecast of circumsolar radiation from whole-sky cameras and satellite sensors. Poster at SolarPACES conference 2016, Abu Dhabi.
5. F.J. Olmo, A. Cazorla, L. Alados-Arboledas, M.A. López-Álvarez, J. Hernández-Andrés, J. Romero, "Retrieval of the optical depth using an all-sky CCD camera", *Applied Optics*, **47**, No.34 (2008).
6. A. Cazorla, J.E. Shields, M.E. Karr, F.J., Olmo, A. Burden, L. Alados-Arboledas, "Technical note: Determination of of aerosol optical properties by a calibrated sky imager", *Atmospheric Chemistry and Physics*, **9**, 6417-6427 (2009).
7. J. Huo and D. Lü, "Preliminary retrieval of aerosol optical depth from all-sky images", *Advances in Atmospheric Sciences*, **27**(2), 421-426 (2010)
8. B. Mayer and A. Kylling, "Technical note: the libRadtran software package for radiative transfer calculations — description and examples of use", *Atmospheric Chemistry and Physics*, **5**, 1855-1877 (2005).